

Quantum energies with worldline numerics

H. Gies and K. Klingmüller

Institute for Theoretical Physics, Philosophenweg 16, D-69120 Heidelberg

E-mail: h.gies@, k.klingmueller@thphys.uni-heidelberg.de

Abstract. We present new results for Casimir forces between rigid bodies which impose Dirichlet boundary conditions on a fluctuating scalar field. As a universal computational tool, we employ worldline numerics which builds on a combination of the string-inspired worldline approach with Monte-Carlo techniques. Worldline numerics is not only particularly powerful for inhomogeneous background configurations such as involved Casimir geometries, it also provides for an intuitive picture of quantum-fluctuation-induced phenomena. Results for the Casimir geometries of a sphere above a plate and a new perpendicular-plates configuration are presented.

1. Introduction

Casimir energies and forces are geometry dependent. Determining the geometry dependence is a challenge both experimentally as well as theoretically. Computing the geometry dependence of Casimir energies can be viewed as a special case of the more general problem of evaluating the effects of quantum fluctuations in a background field $V(x)$. For instance, the space(-time) dependence of the background field can then be used to model the Casimir geometry.

A universal tool to deal with quantum fluctuations in background fields is given by the effective action $\Gamma[V]$ which is the generating functional for 1PI correlation functions for V . In the present work, we consider a fluctuating real scalar quantum field ϕ interacting with the background potential according to $\sim V(x)\phi^2$. For this system, the effective action can be evaluated from

$$\begin{aligned}\Gamma[V] &= -\ln \left(\int \mathcal{D}\phi e^{-\frac{1}{2} \int \phi(-\partial^2 + m^2 + V)\phi} \right) \\ &= \frac{1}{2} \sum_{\lambda} \ln(\lambda^2 + m^2).\end{aligned}\tag{1}$$

Here \hbar and c are set to 1. The integral over the Gaussian fluctuations boils down to a sum over the spectrum $\{\lambda\}$ of quantum fluctuations. This spectrum consists of the eigenvalues of the fluctuation operator,

$$(-\partial^2 + V(x))\phi = \lambda^2 \phi.\tag{2}$$

The relation to Casimir energies becomes most obvious by confining ourselves to time-independent potentials $V(\mathbf{x})$. Then, the sum over the time-like component of the

spectrum can be performed. In Euclidean spacetime, we use $-\partial^2 = -\partial_t^2 - \nabla^2$, $-\partial_t^2 \rightarrow p_t^2$, and the summation/integration over p_t results in

$$E[V] \equiv \frac{\Gamma[V]}{L_t} = \frac{1}{2} \sum \omega, \quad (3)$$

where $\omega^2 = \lambda^2 - p_t^2$ denote the spatial (p_t -independent) part of the fluctuation spectrum. Here, we have defined the Casimir energy from the effective action by dividing out the extent L_t of the Euclidean time direction. The relation to a sum over “ground-state energies” $\sim \frac{1}{2}\hbar\omega$ now becomes obvious.

The general strategy for computing $E[V]$ seems straightforward: determine the spectrum of quantum fluctuations and sum over the spectrum. However, this recipe is plagued by a number of profound problems: first, an analytic determination of the spectrum is possible only in very rare, mainly separable, cases. Second, a numerical determination of the spectrum is generally hopeless, since the spectrum can consist of discrete as well as continuous parts and is generically not bounded. Third, the sum over the spectrum is generally divergent, and thus regularization is required; particularly in numerical approaches, regularization can lead to severe stability problems. And finally, an unambiguous renormalization has to be performed, such that the physical parameters are uniquely fixed.

For a solution of these problems, the technique of *worldline numerics* has been developed [1] and has first been applied to Casimir systems in [2]. This technique is based on the string-inspired approach to quantum field theory [3]. In this formulation, the (quantum mechanical) problem of finding and summing the spectrum of an operator is mapped onto a Feynman path integral over closed worldlines. For the present scalar case, the effective action then reads

$$\Gamma[V] = -\frac{1}{2} \int_{1/\Lambda^2}^{\infty} \frac{dT}{T} e^{-m^2 T} \mathcal{N} \int_{x(T)=x(0)} \mathcal{D}x e^{-\int_0^T d\tau \left(\frac{\dot{x}^2}{4} + V(x(\tau)) \right)}. \quad (4)$$

Now, the effective action, or, more specifically, the Casimir energy, is obtained from an integral over an ensemble of closed worldlines in the given background $V(x)$. This seemingly formal representation can be interpreted in an intuitive manner: A worldline can be viewed as the spacetime trajectory of a quantum fluctuation. The auxiliary integration parameter T is called the proptime and specifies a fictitious “time” which the fluctuating particle has at its disposal for traveling along the full trajectory. Larger values of the proptime thus correspond to worldlines with a larger extent in spacetime; hence, the proptime also corresponds to a smooth regulator scale, with, e.g., short proptimes being related to small-distance UV fluctuations.‡

Most importantly from a technical viewpoint, the problem of finding and summing over the spectrum is replaced by one single step, namely taking the path integral. Moreover, for any given value of proptime T this path integral is finite. Possible UV divergencies can be analyzed with purely analytical means by studying the small- T

‡ For reasons of definiteness, we have therefore cut off the proptime integral at the lower bound at $1/\Lambda^2$ with the UV cutoff scale Λ .

behavior of the proptime integral, and thus no numerical instabilities are introduced by the regularization procedure. The renormalization can be performed in the standard way, for instance, by analyzing the corresponding Feynman diagrams with the same proptime regulator and by fixing the counterterms with the aid of renormalization conditions accordingly.

Further advanced methods which can deal with involved Casimir configurations have been developed during the past years, each with its own respective merits. In particular, we would like to mention the semiclassical approximation [4], a functional-integral approach using boundary auxiliary fields [5], and the optical approximation [6]. These methods are especially useful for analyzing particular geometries by purely or partly analytical means.

Of course, a purely analytical evaluation of the path integral again is only possible for very rare cases, but a numerical evaluation is straightforwardly possible with Monte Carlo techniques and can be realized with conceptually simple algorithms, as described in the next section. Applications to Casimir geometries will be presented in Sect. 3 and conclusions are given in Sec. 4.

2. Worldline numerics for Casimir systems

With the aid of the normalization of the path integral [1], we note that (4) can be written as

$$\Gamma[V] = -\frac{1}{2} \frac{1}{(4\pi)^2} \int_{1/\Lambda^2}^{\infty} \frac{dT}{T^3} e^{-m^2 T} \left(\left\langle e^{-\int_0^T d\tau V(x(\tau))} \right\rangle_x - 1 \right), \quad (5)$$

where the subtraction of -1 ensures that $\Gamma[V = 0] = 0$. The expectation value in (5) has to be taken with respect to the worldline ensemble,

$$\langle \dots \rangle := \left(\int_{x(T)=x(0)} \mathcal{D}x \dots e^{-\frac{1}{4} \int_0^T d\tau \dot{x}^2} \right) \left(\int_{x(T)=x(0)} \mathcal{D}x e^{-\frac{1}{4} \int_0^T d\tau \dot{x}^2} \right)^{-1}. \quad (6)$$

In the present work, we focus on the “ideal” Casimir effect induced by real scalar field fluctuations obeying Dirichlet boundary conditions; i.e., the boundary conditions are satisfied at infinitely thin surfaces. This situation can be modeled by choosing $V(x) = g \int_{\Sigma} d\sigma \delta^{(4)}(x - x_{\sigma})$, where $d\sigma$ denotes the integration measure over the surface Σ , with x_{σ} being a vector pointing onto the surface. The Dirichlet boundary condition is then strictly imposed by sending the coupling g to infinity, $g \rightarrow \infty$ [7, 8].

Moreover, we are finally aiming at Casimir forces between disconnected rigid surfaces, which can be derived from the Casimir interaction energy,

$$E_{\text{Casimir}} = E[V_1 + V_2] - E[V_1] - E[V_2], \quad (7)$$

where we subtract the Casimir energies of the single surfaces V_1 and V_2 from that of the combined configuration $V_1 + V_2$;§ the former do not contribute to the force. This

§ Alternatively, the single-surface subtraction terms in (7) can be viewed as subtracting the Casimir energy for the surfaces at infinite separation.

definition, together with the Dirichlet boundary condition, leads to

$$E_{\text{Casimir}} = -\frac{1}{2} \frac{1}{(4\pi)^2} \int_0^\infty \frac{dT}{T^3} e^{-m^2 T} \langle \Theta_V[x] \rangle_x, \quad (8)$$

where $\Theta_V[x] = 1$ if a given worldline intersects both surfaces $\Sigma = \Sigma_1 + \Sigma_2$ represented by the background potentials $V = V_1 + V_2$, and $\Theta_V[x] = 0$ otherwise. This recipe has a simple interpretation: any worldline which intersects both surfaces corresponds to a quantum fluctuation that violates the Dirichlet boundary conditions. Its “removal” from the set of all fluctuations contributes “one unit” to the negative Casimir interaction energy.

The worldline numerical algorithm is based on an approximation of the path integral by a sum over a finite ensemble of n_L number of paths, each of which is characterized by N discrete points per loop (ppl). These points are obtained by a discretization of the proper-time parameter on each loop, $x_i = x(\tau_i)$, $i = 1, \dots, N$, with $(x_i)_\mu \in \mathbb{R}$. For an efficient generation of the worldline ensemble which obeys a Gaussian velocity distribution required for (6), various algorithms are available, see [2, 9].

In summary, worldline numerics offers a number of advantages: first, the whole algorithm is independent of the background; no particular symmetry is required. Second, the numerical cost scales only linearly with the parameters n_L , N , and the dimensionality of the problem. The numerically most expensive part of the calculation is a diagnostic routine that detects whether a given worldline intersects both surfaces or not, returning the value $\Theta_V[x] = 1$ or 0, respectively. Optimizing this diagnostic routine for a given geometry can lead to a significant reduction of numerical costs. Details of this optimization for the geometries considered below will be given elsewhere [10].

3. Application to Casimir geometries

3.1. Sphere above plate

The geometry of a sphere above a plate is the most relevant configuration as far as recent and current experiments are concerned [11]. Therefore, also worldline numerics has first been applied to this case [2]. Here we extend these studies, arriving at significantly improved results with much smaller error bars and for a wider range of parameters. In the following, we exclusively discuss the massless case, $m = 0$.

It is interesting to compare our results to the proximity force approximation (PFA) [12] which is the standard tool for estimating the effects of departure from planar geometry for Casimir effects. In this approach, the curved surfaces are viewed as a superposition of infinitesimal parallel plates, and the interaction energy is then obtained by

$$E_{\text{PFA}} = \int_{\Sigma_{\text{PFA}}} E_{\text{PP}}(d) d\sigma. \quad (9)$$

Here, Σ_{PFA} denotes a “suitable” auxiliary surface in between the Casimir surfaces Σ_1 and Σ_2 , and $d\sigma$ is the corresponding surface element of Σ_{PFA} . The distance d between

two points on Σ_1 and Σ_2 has to be measured along the normal to Σ_{PFA} . Obviously, the definition of E_{PFA} is ambiguous, owing to possible different choices of Σ_{PFA} . The two extreme cases are $\Sigma_{\text{PFA}} = \Sigma_1$ or $\Sigma_{\text{PFA}} = \Sigma_2$. The difference in E_{PFA} for these two cases is considered to represent a rough error estimate of the PFA. In the above formula, E_{PP} denotes the classic parallel-plate result for the energy per unit area A [13],

$$\frac{E_{\text{PP}}(a)}{A} = -c_{\text{PP}} \frac{\pi^2}{1440} \frac{1}{a^3}, \quad (10)$$

with a denoting the plate separations, and $c_{\text{PP}} = 2$ for an electromagnetic (EM) field or a complex scalar, and $c_{\text{PP}} = 1$ for the present case of a real scalar field fluctuation.

For the configuration of a sphere above a plate, we can choose Σ_{PFA} equal to the plate (plate-based PFA), or equal to the sphere (sphere-based PFA) as the extreme cases. The corresponding results of the integral of (9) can be given in closed form, see, e.g., [6]. In the limit of small distances a compared to the sphere radius R , $a/R \ll 1$, both PFA's agree,

$$E_{\text{PFA}}(a/R \ll 1) = -c_{\text{PP}} \frac{\pi^3}{1440} \frac{R}{a^2}. \quad (11)$$

It is useful to display the resulting Casimir energies normalized to this zeroth-order small-separation PFA limit as it is done in figure 1. The dashed and dot-dashed lines depict the plate-based and sphere-based PFA, respectively. For larger separations, both cases predict a decrease of the Casimir energy relative to the zeroth-order PFA in (11).

Our numerical worldline estimate confirms the zeroth-order PFA in the limit of small a/R . But in contrast to the PFA curves, worldline numerics predicts a relative increase of the Casimir energy in comparison with (11) for larger separations/smaller spheres. We conclude that the PFA should not at all be trusted beyond the zeroth order: the first-order correction does not even have the correct sign. As a most conservative estimate, we observe that the PFA deviates from our result by at least 1% for $a/R > 0.01$, which confirms and strengthens the result of [2]. A more detailed investigation of the validity bounds of the PFA will be given elsewhere [10]. It is interesting to observe that the zeroth-order PFA (11) still seems to be a reasonable estimate up to $a/R \simeq 0.1$, indicating that the true curvature effects compensate for the higher-order PFA corrections.

Finally, we note that our results agree with the optical approximation [6] for $a/R \lesssim 0.1$, confirming the absence of diffractive effects in this regime, which are neglected by the optical approximation. For even larger separations a , we observe a monotonous increase of the Casimir energy relative to (11). In this regime, our results agree quantitatively with those obtained from the ‘‘KKR’’ multi-scattering map method presented by A. Wirzba at this QFEXT05 workshop [14]. Most importantly, we do not observe a Casimir-Polder law for large a/R , which would manifest itself in an $(a/R)^{-2}$ decrease in figure 1 at the large- (a/R) side. Since a Casimir-Polder law is expected for the electromagnetic case, our results for the Dirichlet scalar provide clear evidence for the fact that the relation between Casimir forces for the EM field and for the Dirichlet scalar is strongly geometry dependent. In fact, the latest results of Ref.[14] include an

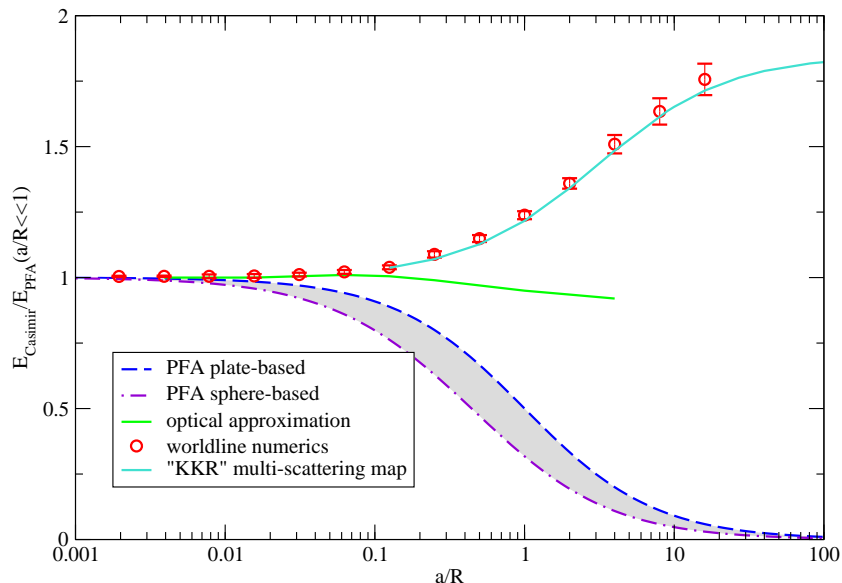


Figure 1. Casimir energy for the sphere-plate configuration normalized to the zeroth-order PFA formula (11): the dashed and dot-dashed lines depict the plate-based and the sphere-based PFA estimates, respectively. The circle symbols display our worldline numerical result. The deviation from the PFA estimate characterizes the relevance of Casimir curvature effects. Also shown is the result from the optical approximation [6], which, within its validity limits $a/R \lesssim 0.1$, agrees well with our result. For larger a/R , we find satisfactory agreement with the "KKR" multi-scattering map method presented at this workshop [14].

analytic proof that the energy ratio of Fig. 1 approaches a constant, $180/\pi^4 \simeq 1.848$ for large a/R for the Dirichlet scalar. The analysis of the sphere-plate configuration for the EM field therefore still remains an open unsolved problem. Note that this does not affect our conclusions about the PFA, since also the PFA does not treat the EM case or the Dirichlet scalar in a different manner.

3.2. Perpendicular plates

A particularly inspiring geometry is given by a variant of the classic parallel-plate case: a semi-infinite plate perpendicular to an infinite plate, such that the edge of the semi-infinite plate has a minimal distance a to the infinite plate, see figure 2 (left panel). Whereas Casimir's parallel-plate case has only one nontrivial direction (the one normal to the plates), this perpendicular-plates case has two nontrivial directions but still only one dimensionful scale a . This fixes the scale dependence of the energy per unit length unambiguously,

$$\frac{E_{\perp}(a)}{L_{\text{T}}} = -\gamma_{\perp} \frac{\pi^2}{1440} \frac{1}{a^2}, \quad (12)$$

where L_{T} denotes the extent of the system along the remaining trivial transversal direction. The unknown coefficient γ_{\perp} results from the effect of quantum fluctuations

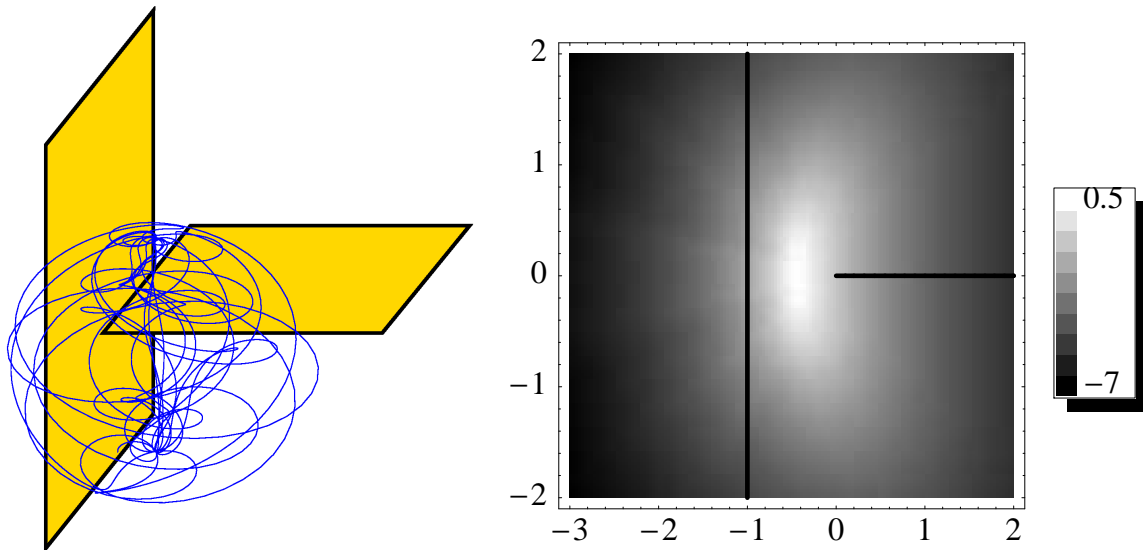


Figure 2. Left panel: sketch of the perpendicular-plates configuration with (an artist's view of) a typical worldline that intersects both plates. Right panel: density plot of the effective action density \mathcal{L} for the perpendicular plates case; the plot shows $\ln(2(4\pi a^2)^2|\mathcal{L}|)$. The position of the perpendicular plates are indicated by solid lines for illustration.

in this geometry and will be determined by worldline numerics.

Let us first note that the PFA does not appear to be useful for the perpendicular-plates case, because the surfaces cannot reasonably be subdivided into infinitesimal surface elements facing each other from plate to plate. For instance, choosing either of the plates as the integration surface in (9), the PFA would give a zero result. However, in the worldline picture, it is immediately clear that the interaction energy is nonzero, because there are many worldlines which intersect both plates, as sketched in figure 2 (left panel). As a direct evidence, we plot the negative effective action density \mathcal{L} (effective Lagrangian) in figure 2 (right panel); the effective action is obtained from $\Gamma = \int d^4x \mathcal{L}$. Brighter areas denote a higher density of the center-of-masses of those worldlines which intersect both plates.

Integrating over the effective action density, we obtain the universal coefficient

$$\gamma_{\perp} = 0.87511 \pm 0.00326, \quad (13)$$

using $n_L = 40000$ worldlines with $N = 200000$ ppl generated by the *v loop* algorithm [2].

4. Conclusions

We have presented new results for interaction Casimir energies, giving rise to Casimir forces between rigid bodies, induced by a fluctuating real scalar field that obeys Dirichlet boundary conditions. We have used worldline numerics as a universal tool for dealing with quantum fluctuations in inhomogeneous backgrounds.

For the experimentally relevant sphere-plate configuration, we have performed extensive numerical studies, confirming earlier findings [2] with a significantly higher precision and narrowing the validity bounds of the proximity force approximation even further. Moreover, our results for small spheres for the Dirichlet scalar shows no sign of a Casimir-Polder law, as it would be expected for the EM field. This provides clear evidence for a different role of Casimir curvature effects for these two different field theories, leaving the sphere-plate configuration with a fluctuating EM field as a pressing open problem.

Furthermore, we have investigated a new geometry of two perpendicular plates which has been inaccessible so far for other approximation techniques. The configuration is representative for a whole new class of Casimir systems involving sharp edges, where diffractive portions of the fluctuating field will play a major role.

Acknowledgments

It is a pleasure to thank Emilio Elizalde and his team for the organization of this workshop and for creating such a stimulating atmosphere. H.G. acknowledges useful discussions with G.V. Dunne, T. Emig, A. Scardicchio, O. Schröder, A. Wirzba, and H. Weigel. This work was supported by the Deutsche Forschungsgemeinschaft (DFG) under contract Gi 328/1-3 (Emmy-Noether program) and Gi 328/3-2.

References

- [1] H. Gies and K. Langfeld, Nucl. Phys. B **613**, 353 (2001); Int. J. Mod. Phys. A **17**, 966 (2002).
- [2] H. Gies, K. Langfeld and L. Moyaerts, JHEP **0306**, 018 (2003); arXiv:hep-th/0311168.
- [3] For a review, see C. Schubert, Phys. Rept. **355**, 73 (2001).
- [4] M. Schaden and L. Spruch, Phys. Rev. A **58**, 935 (1998); Phys. Rev. Lett. **84** 459 (2000)
- [5] R. Golestanian and M. Kardar, Phys. Rev. A **58**, 1713 (1998); T. Emig, A. Hanke and M. Kardar, Phys. Rev. Lett. **87** (2001) 260402; T. Emig and R. Buscher, Nucl. Phys. B **696**, 468 (2004).
- [6] A. Scardicchio and R. L. Jaffe, Nucl. Phys. B **704**, 552 (2005); Phys. Rev. Lett. **92**, 070402 (2004).
- [7] M. Bordag, D. Hennig and D. Robaschik, J. Phys. A **25**, 4483 (1992).
- [8] N. Graham, R. L. Jaffe, V. Khemani, M. Quandt, M. Scandurra and H. Weigel, Nucl. Phys. B **645**, 49 (2002).
- [9] H. Gies, J. Sanchez-Guillen and R. A. Vazquez, JHEP **0508**, 067 (2005).
- [10] H. Gies and K. Klingmuller, arXiv:quant-ph/0601094.
- [11] S. K. Lamoreaux, Phys. Rev. Lett. **78**, 5 (1997); U. Mohideen and A. Roy, Phys. Rev. Lett. **81**, 4549 (1998); H. B. Chan, V. A. Aksyuk, R. N. Kleiman, D. J. Bishop and F. Capasso, Science **291**, 1941 (2001); R.S. Decca, D. Lopez, E. Fishbach, D.E. Krause, Phys. Rev. Lett., **91**, (2003), 050402.
- [12] B.V. Derjaguin, I.I. Abrikosova, E.M. Lifshitz, Q.Rev. **10**, 295 (1956); J. Blocki, J. Randrup, W.J. Swiatecki, C.F. Tsang, Ann. Phys. (N.Y.) **105**, 427 (1977).
- [13] H. B. Casimir, Kon. Ned. Akad. Wetensch. Proc. **51**, 793 (1948).
- [14] A. Wirzba, A. Bulgac and P. Magierski, Proceedings of the workshop QFEXT05 (2005), arXiv:quant-ph/0511057; A. Bulgac, P. Magierski and A. Wirzba, Phys. Rev. D **73**, 025007 (2006).